Synthon polymorphs of sulfacetamide−acetamide cocrystal based on N−H···O=S and N−H···O=C hydrogen bonding†

N. Rajesh Goud, and Ashwini Nangia*

School of Chemistry, University of Hyderabad, Prof. C.R. Rao Road, Gachibowli, Central University PO, Hyderabad 500 046, India. E-mail: ashwini.nangia@gmail.com

Electronic Supplementary Information†

Table S1 List of polymorphic molecules with the SO_2-NH-CO fragment in Organic crystal structures retrieved from the Cambridge Structural Database (CSD, ver. 5.34, Conquest 1.15, November 2012 release).

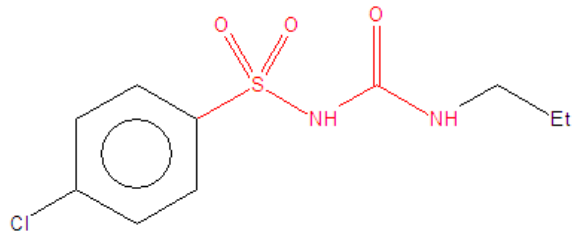 Chlorpropamide, BEDMIG	5 polymorphs
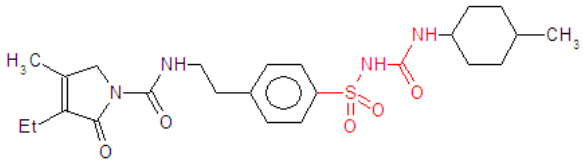 Glimepiride, TOHBUN	2 polymorphs
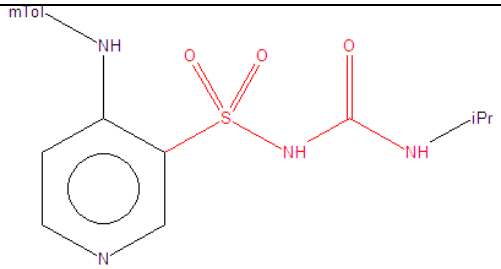 Torasemide, TORSEM	3 polymorphs
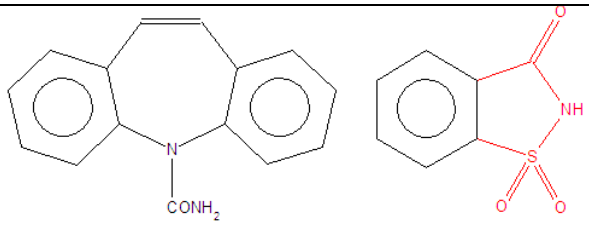 Carbamazepine-Saccharin, UNEZAO	2 polymorphs

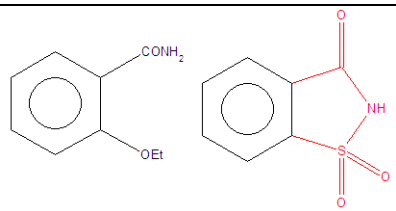 Ethenzamide-Saccharin, VUHFIO	2 polymorphs
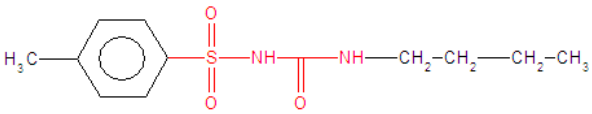 Tolbutamide, ZZZPUS	6 polymorphs

Table S2 Hydrogen bond synthon patterns (rings, chains, etc.) in polymorphic compounds with the SO_2NHCO functional group (listed in Table S1).

Chlorpropamide – 5 polymorphs	
$P2_1$ 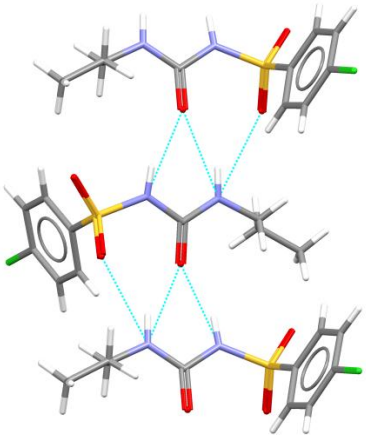 Urea tape-motif, with one of the hydrogen atom in the tape bifurcating to form N–H⋯O=S H-bond	Pbcn 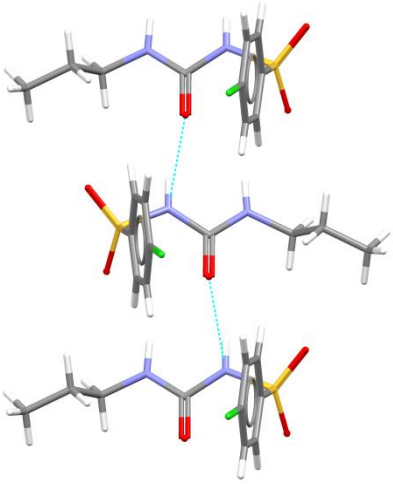 Catemeric N–H⋯O=C H-bond

Pbca 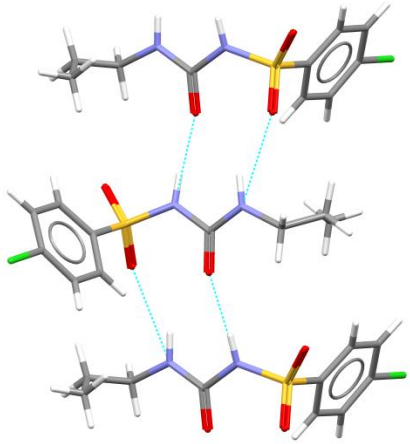 Two point synthon comprised of N–H···O=C and N–H···O=S H-bonds	$Pna2_1$ 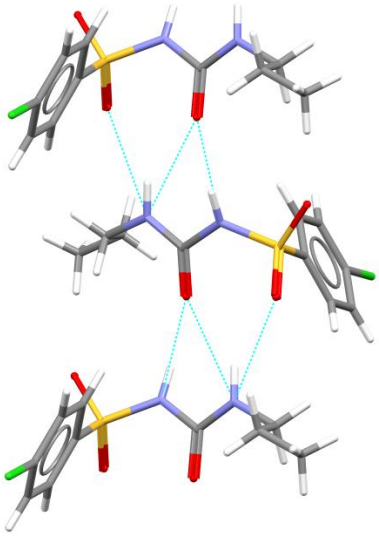 Synthon similar to $P2_1$ structure
$P2_12_12_1$ 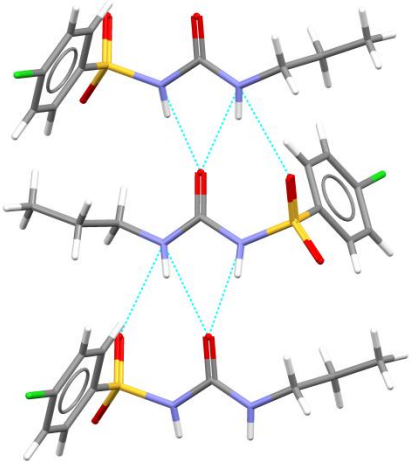 Synthon similar to $P2_1$ structure	
Glimepiride – 2 polymorphs	

Pbca 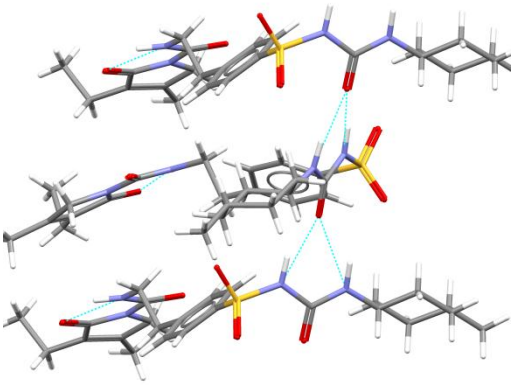 Urea-tape motif	$P2_1/n$ 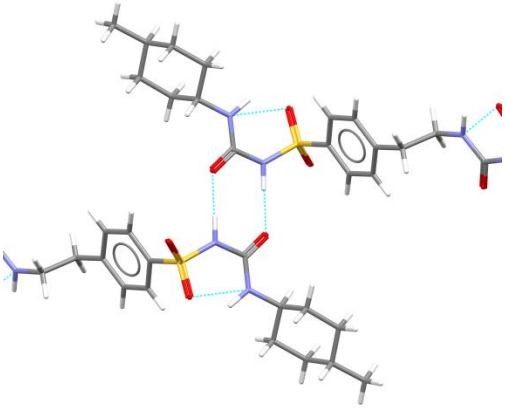 Carboxamide dimer
Torasemide – 3 polymorphs	
$P2_1/c$ 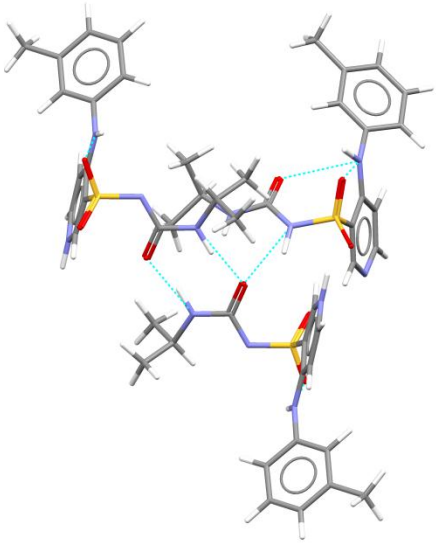 Carboxamide dimer and catemer	P2/n 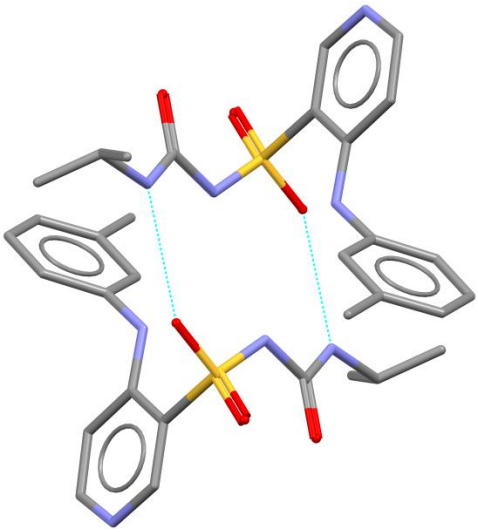 N–H⋯O=S dimer ring motif

$P2_1/c$ 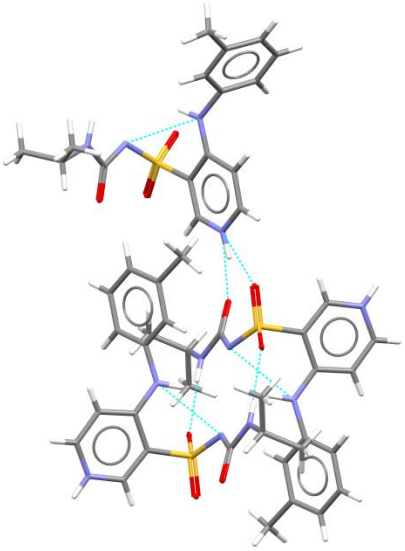 Zwitterionic polymorph N–H⋯O=S dimer type along with bifurcated N–H⋯C=O and N–H⋯S=O H-bonds	
Tolbutamide – 3 polymorphs	
$P2_1/n$ 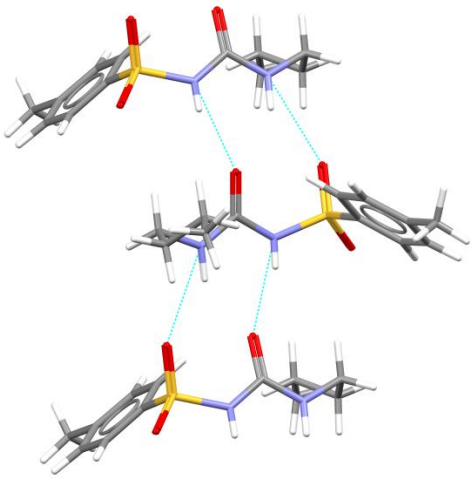 Cyclic synthon of N–H⋯O=C and N–H⋯O=S H-bonds	$P2_1/c$ 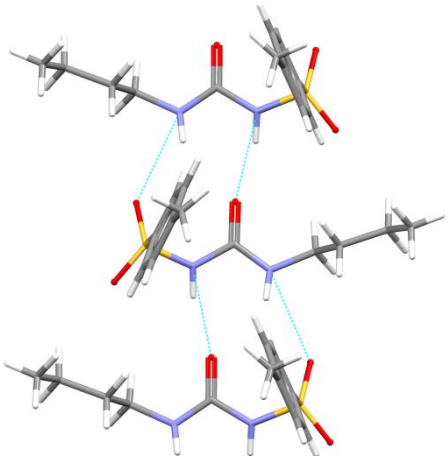 Cyclic motif of N–H⋯O=C and N–H⋯O=S H-bonds

Pbcn 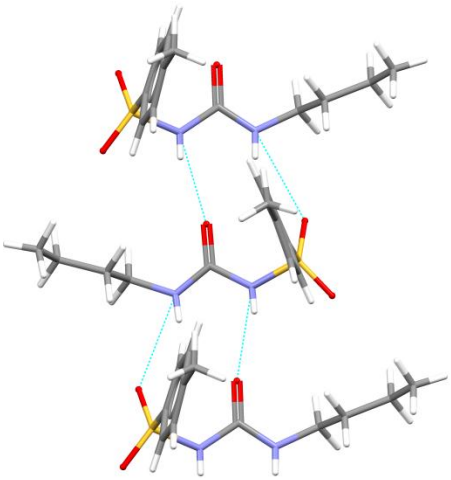 Cyclic synthon of N–H···O=C and N–H···O=S H-bonds	
Ethenzamide−saccharin cocrystal – 2 polymorphs	
P-1 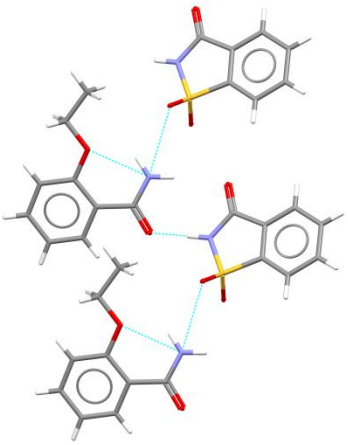 Catemer N–H···O=C and N–H···O=S H-bonds	P21/c 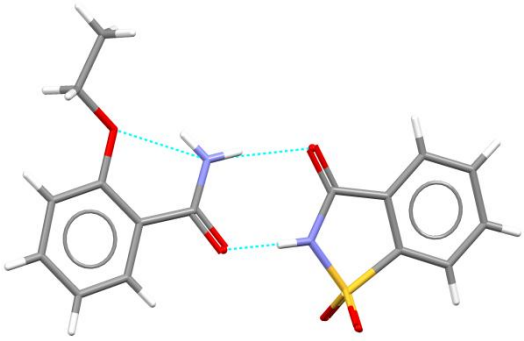 Carboxamide dimer synthon

Carbamazepine−saccharin cocrystal	
P-1 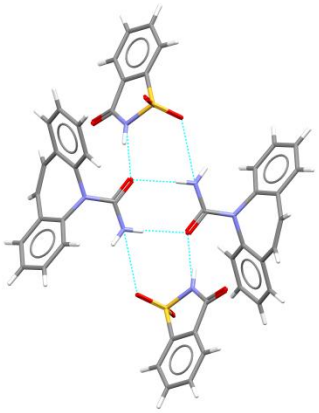 Carboxamide homodimer along with N–H···O=S H-bond with saccharin	$P2_1/c$ 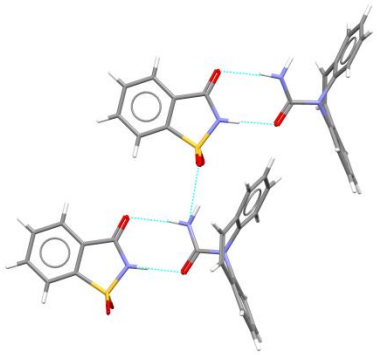 N–H···O=S and N–H···O=C heterodimer

Table S3 CSD Refcodes of neutral polymorphic cocrystals retrieved from the last full release of the CSD, ver. 5.34, Conquest 1.15, November 2012 release).

Entry	Cocrystal Polymorph	REFCODEs
1	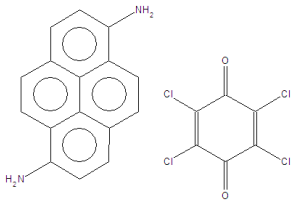	ABEKUN ABEKUN01 ABEKUN02
2	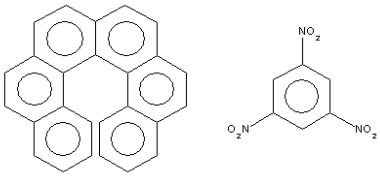	ABUNIU ABUNIU01
3	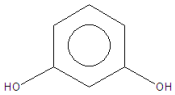 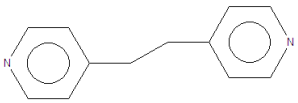	ACOYOG ACOYOG01

4	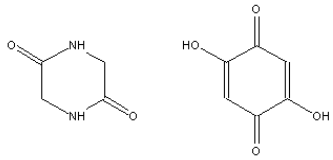	AJAJEA AJAJEA01
5	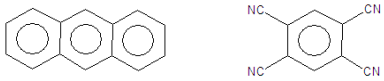	ANTCYB, ANTCYB12 ANTCYB11 ANTCYB13 ANTCYB14 ANTCYB15 ANTCYB16
6	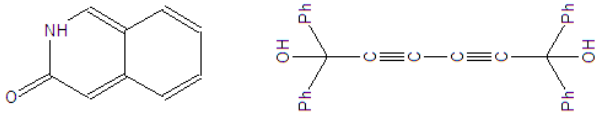	ANUMEC ANUMEC01
7	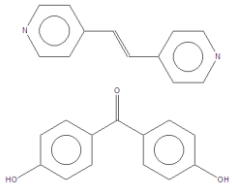	BIVSIJ01 BIVSIJ02
8	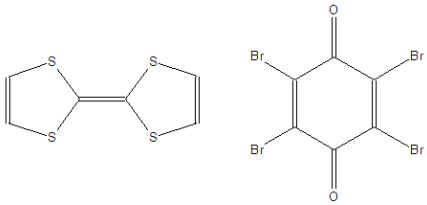	CAZLAR, CAZLAR01 CAZLAR02
9	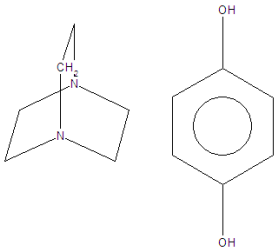	COHWIF, COHWIF02, COHWIF03 COHWIF01
10	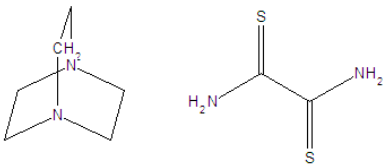	DOKGUG DOKGUG01

11	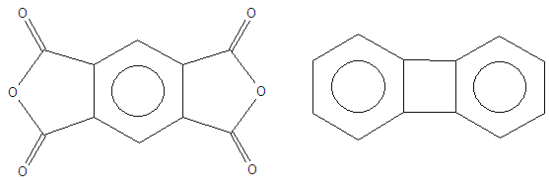	DURZAR DURZAR01
12	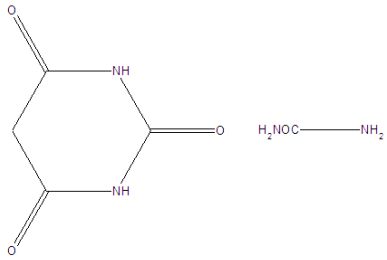	EFOZAB, EFOZAB03 EFOZAB01 EFOZAB04 EFOZAB02
13	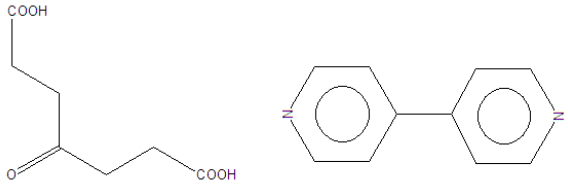	ELEGUY ELEGUY01
14	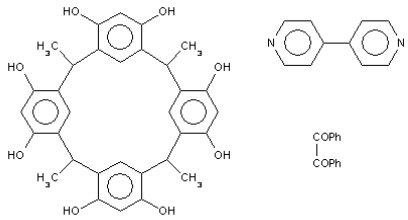	ENAZOI ENAZOI01
15	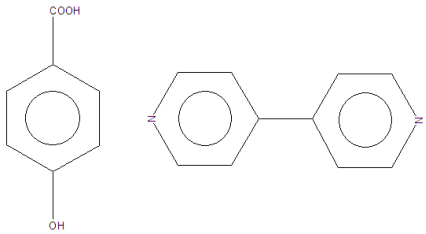	EPUPUB EPUPUB01
16	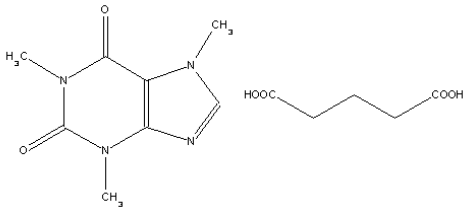	EXUQUJ EXUQUJ01
17	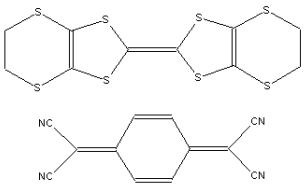	FAHLEF01 FAHLEF02

18	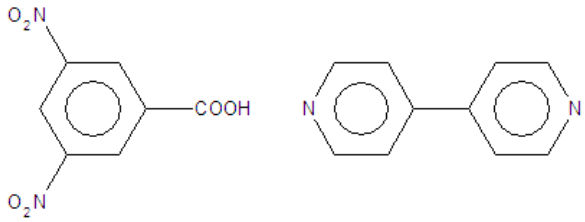	FIHYEA FIHYEA02
19	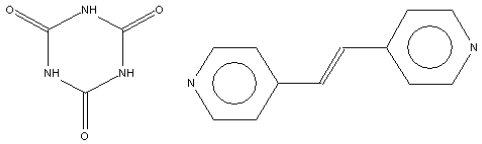	HADKUT HADKUT01
20	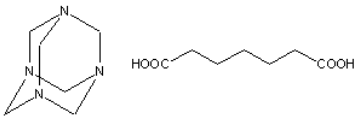	IJETOG IJETOG02
21	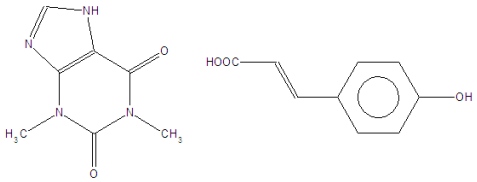	IJIBEJ IJIBEJ01
22	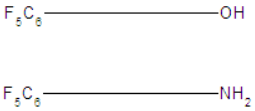	KIBQOC KIBQOC01
23	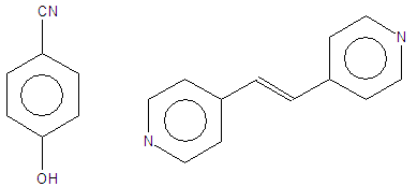	KIHYOQ KIHYOQ01
24	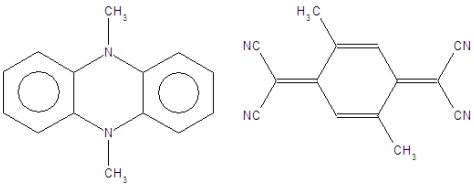	LOCVOO LOCVOO01

25	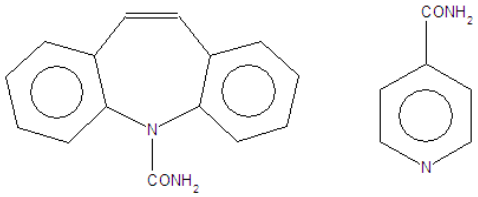	LOFKIB LOFKIB01
26	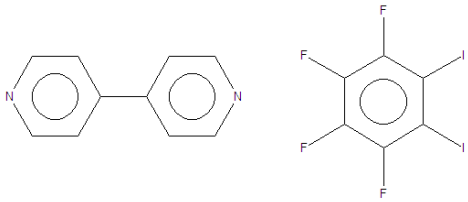	MIYKOU MIYKOU01
27	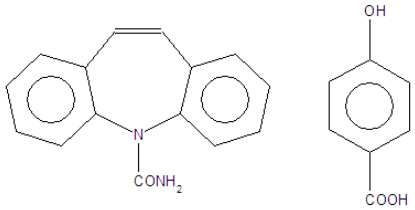	MOXVIF MOXVIF01
28	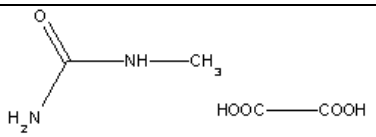	MUROXA MUROXA01
29	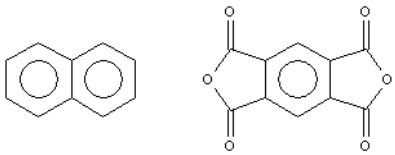	NAPYMA NAPYMA01
30	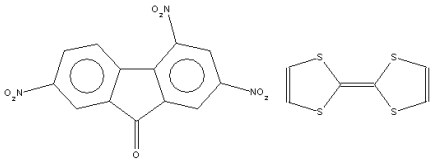	NARSOP NARSOP01 NARSOP02
31	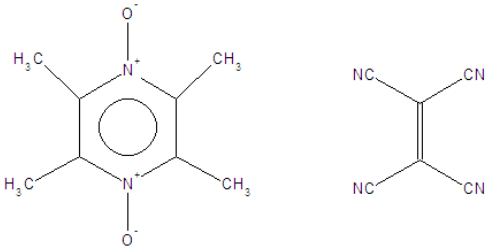	NITRIR NITRIR01

32	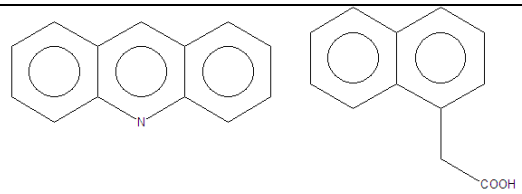	NOVSIA NOVSIA01
33	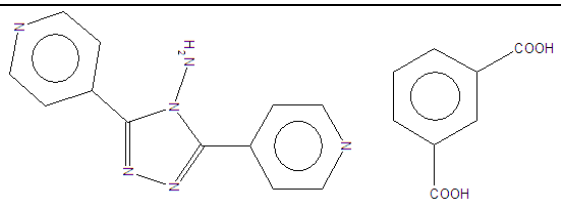	NUGZEV NUGZEV01
34	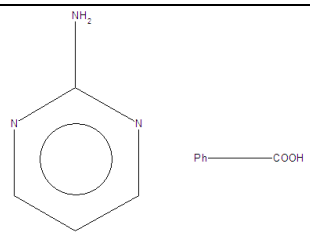	NUKWEW NUKWEW01
35	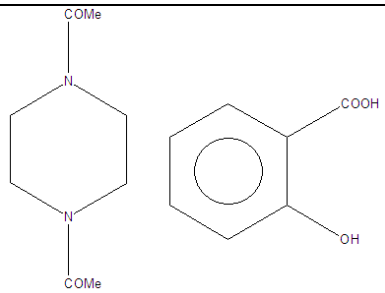	NUKXEX NUKXEX01
36	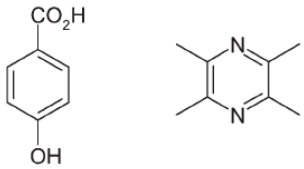	ODOBIT ODOBIT01
37	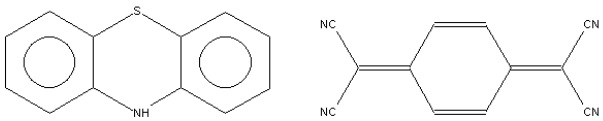	PTZTCQ PTZTCQ01
38	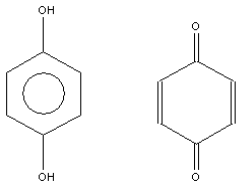	QUIDON QUIDON01 QUIDON02

39	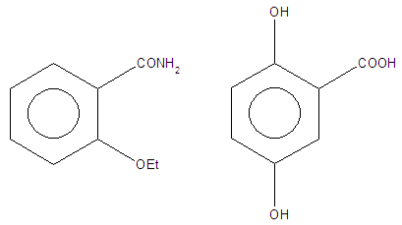	QULLUF QULLUF01 QULLUF02
40	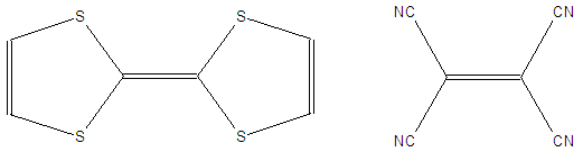	RIFQAY RIFQAY01
41	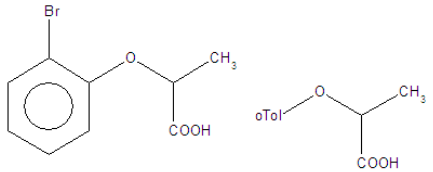	RIWWEA RIWWEA01
42	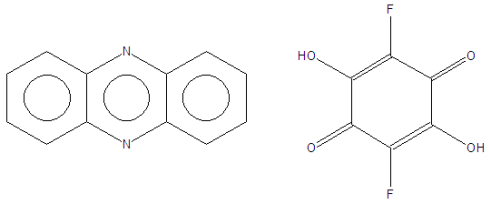	RURROM RURROM01
43	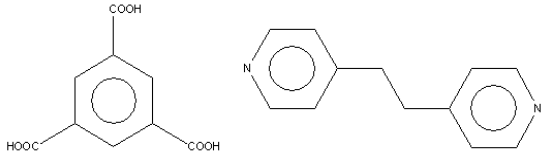	SAYMUB SAYMUB01
44	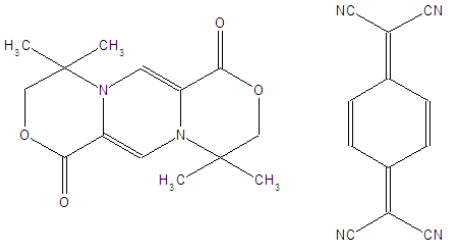	TAMBUE TAMBUE01
45	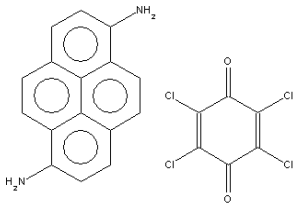	TECCAF01 TECCAF02

46	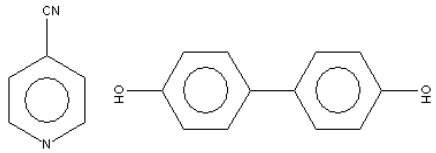	TEHNAW TEHNAW01
47	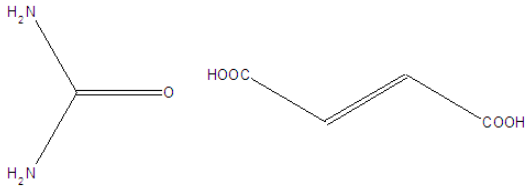	TIPWIY TIPWIY01
48	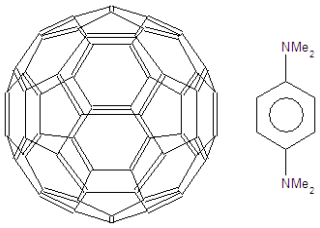	TONDUV TONDUV02
49	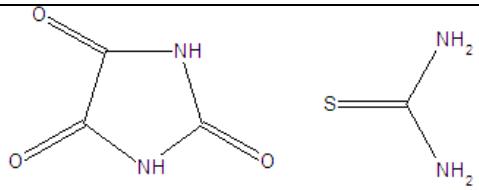	TUPRBN01 TUPRBN10
50	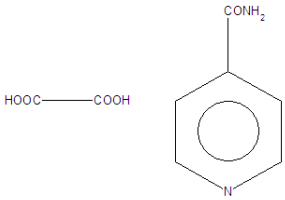	ULAWAF ULAWAF01 ULAWAF02
51	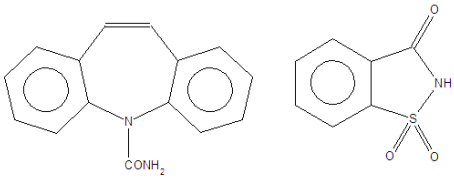	UNEZAO UNEZAO01
52	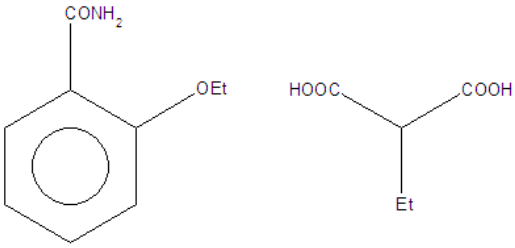	VAKTOS VAKTOS01

53	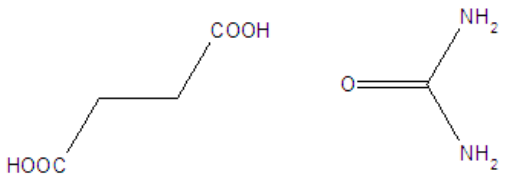	VEJXAJ VEJXAJ01
54	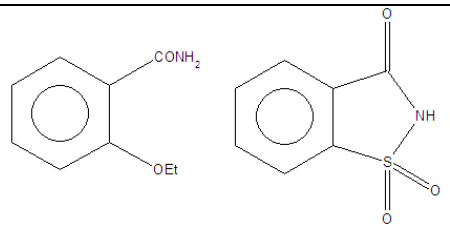	VUHFIO VUHFIO01
55	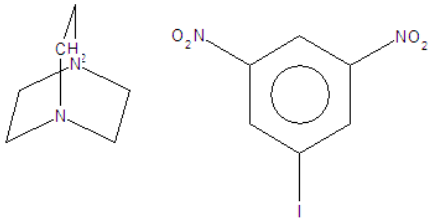	VUJSOJ VUJSOJ01
56	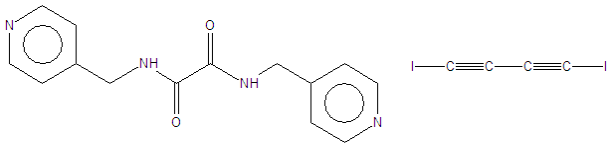	WANNUV WANNUV01
57	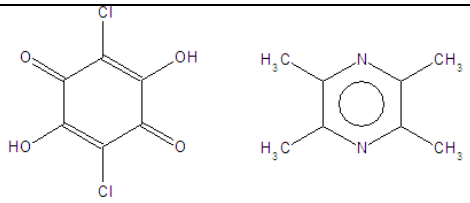	WATREP, WATREP01 WATREP04 WATREP02 WATREP03
58	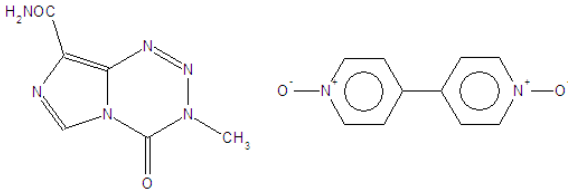	WOBQEK WOBQEK01
59	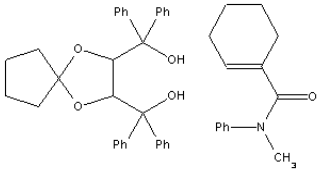	WOTZAG WOTZAG01

60	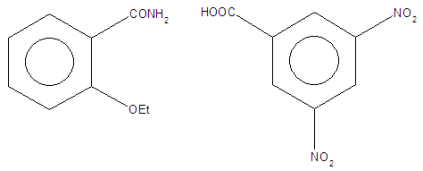	WUZHOP WUZHOP01
61	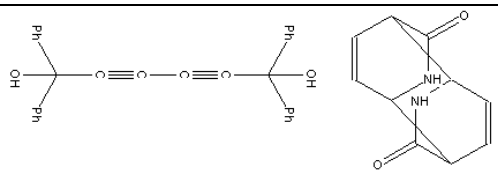	XETZIG XETZIG01
62	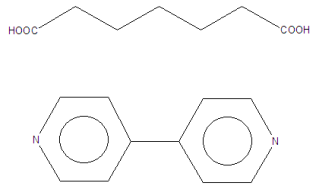	XOLHUC XOLHUC01 XOLHUC02
63	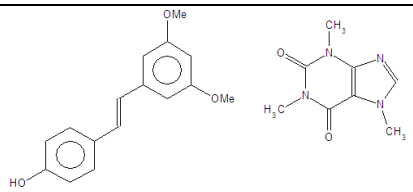	YABHAM YABHAM01
64	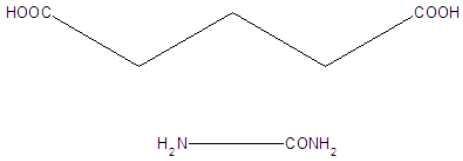	ZODWIY ZODWIY01
65	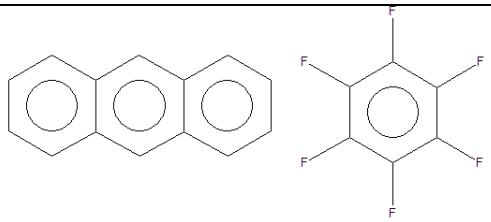	ZZZGMW01 ZZZGMW02
66	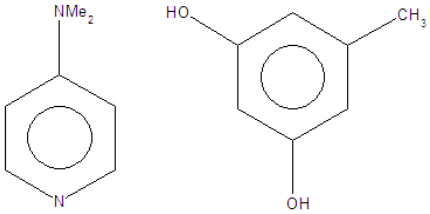	EWAPAU EWAPAU01

67	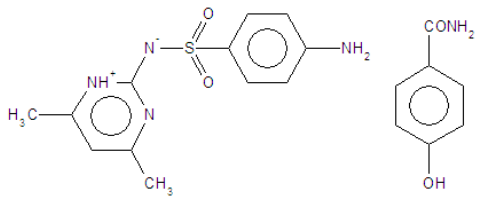	EXAPID EXAPID01
68	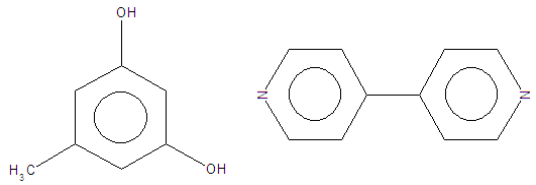	UBUJIM UBUJIM01
69	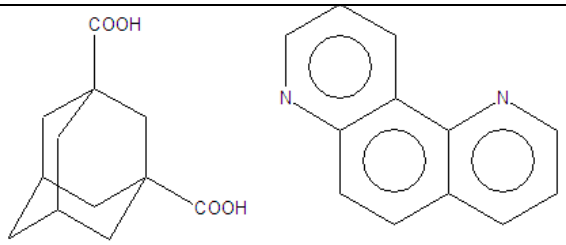	PANQUS PANQUS01
70	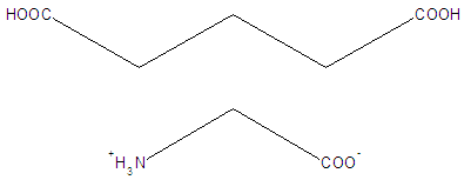	AWIHOE02 AWIHOE03 AWIHOE04 AWIHOE05 AWIHOE06 AWIHOE07 AWIHOE08 AWIHOE09 AWIHOE10
71	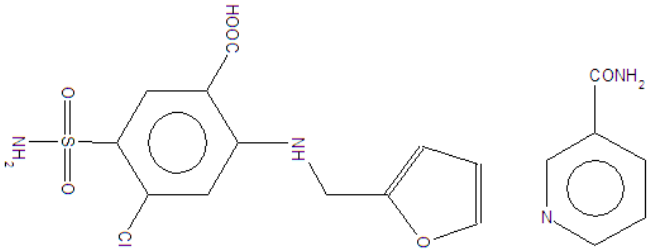	YASGOQ YASGOQ01 YASGOQ02 YASGOQ03
72	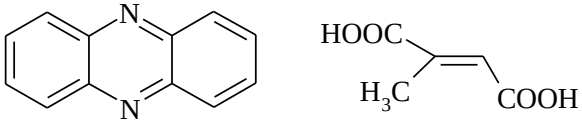	WOQBAF WOQBAF01

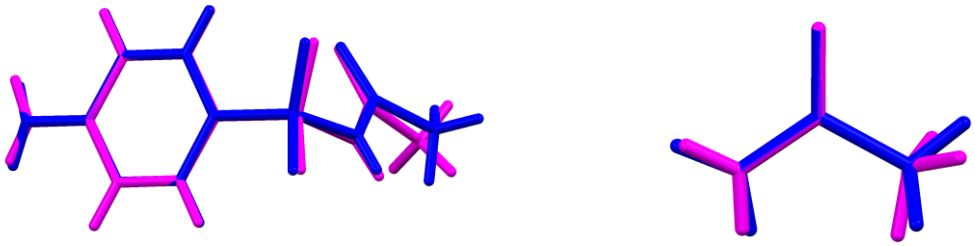

Fig. S1 Overlay of SACT and ACT molecules in cocrystal form 1 (blue) and 2 (magenta).

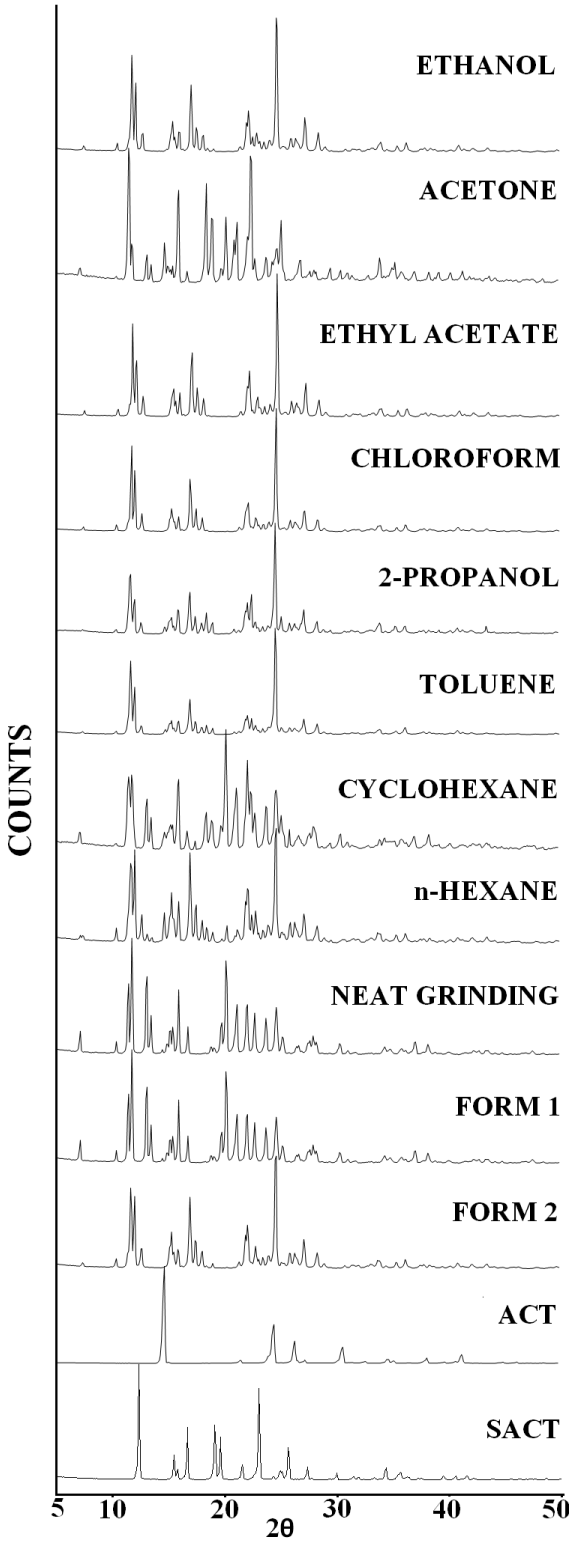

Fig. S2 Comparison of PXRD patterns of the samples obtained in the grinding experiments of 1:1 mixture of SACT and ACT. Solvent used in grinding experiments is indicated on the right. The resulting powder pattern did not follow any trend based on the polarity of solvent used.

Table S4 ss-NMR ^{13}C chemical shifts (δ, ppm) of SACT−ACT cocrystal polymorphs.

Carbon No.	SACT-ACT-FORM-1	SACT-ACT-FORM-2
8	20.8	20.3
10	24.4	25.4
2,6	112.9	111.4, 113.2
4	123.1	120.2
5	129.3	127.5
3	134.3	132.7
1	154.6	154.5
9	172.8	173.5
7	175.3	175.8

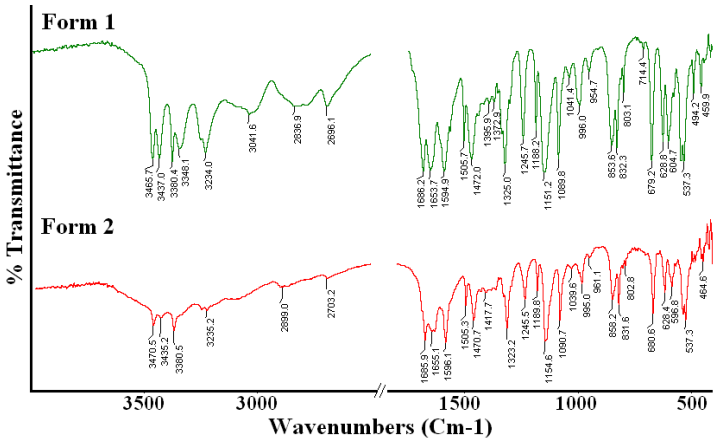

(a)

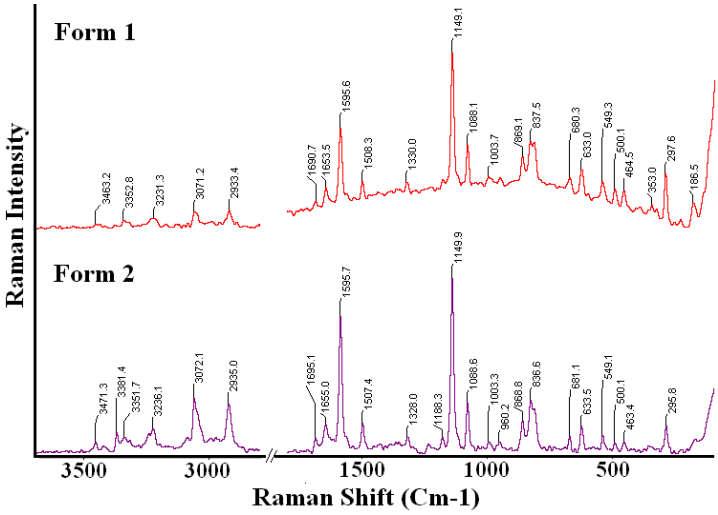

(b)

Fig. S3 IR and Raman spectra of SACT-ACT cocrystal polymorphs.

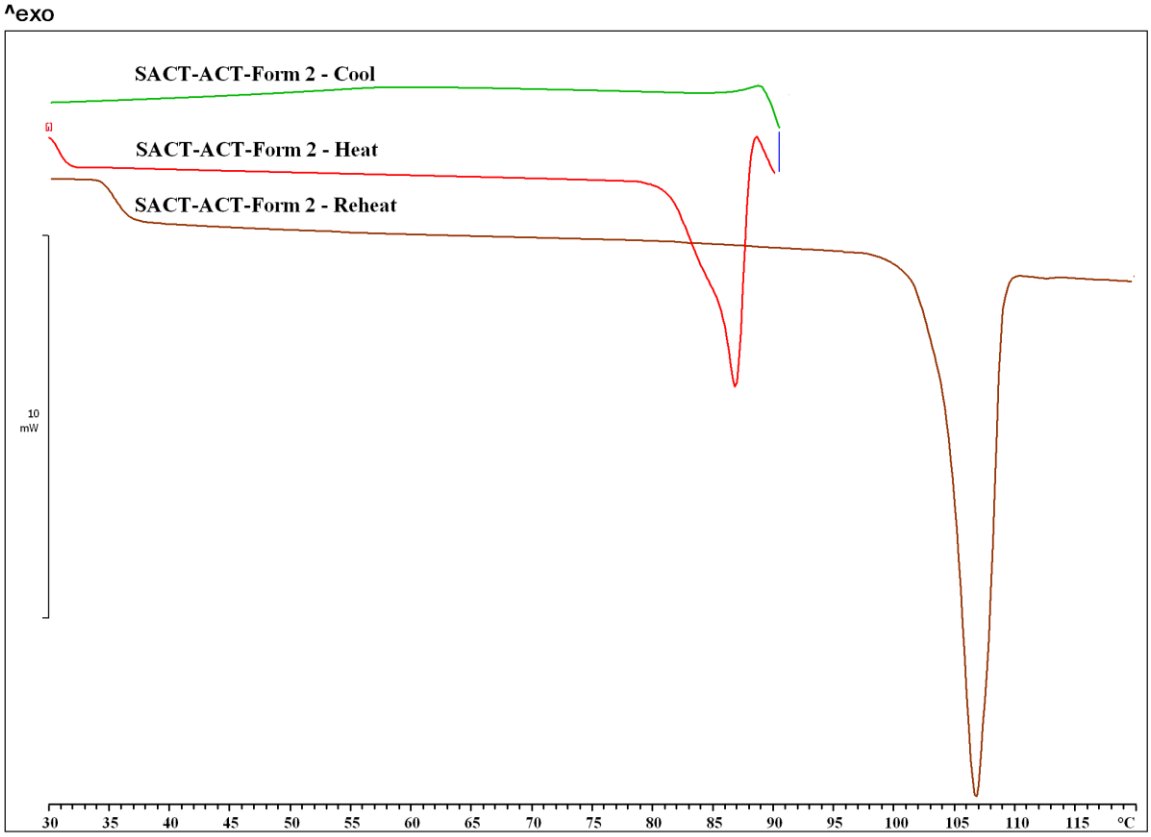

Fig. S4 Heat-cool-heat DSC heating curve of SACT-ACT Form 2 indicated that the high temperature phase is form 1.

Eqn. S1 Calculation of melting point of SACT−ACT metastable form 2 (taken from ref. 15).

$$T_{fus(form\,2)} = \frac{\Delta H_{fus(form\,2)} \times T_{fus(form\,1)} \times T_{trs}}{(\Delta H_{fus(form\,2)} \times T_{fus(form\,1)}) + (T_{trs} \times \Delta H_{fus(form\,1)}) - (T_{fus(form\,1)} \times \Delta H_{fus(form\,1)})}$$

$$T_{fus(form\,2)} = \frac{32.3 \times 106.5 \times 79}{(106.5 \times 32.3) + (79 \times 29.5) - (106.5 \times 29.5)} = 103.4°\,C$$

ΔH_{fus} (form 2) = Enthalpy of fusion of form 2 (Enthalpy of fusion of form 1 + Enthalpy of Transition) = 32.3 kJ/mol

T_{fus} (form 1) = Temperature of fusion of form 1 = 106.5°C

T_{trs} = Temperature of transition from form 2 to form 1 = 79°C

ΔH_{fus} (form 1) = Enthalpy of fusion of form 1 = 29.5 kJ/mol
T_{fus} (form 2) = Temperature of fusion of form 2 (calculated) = 103.4°C

Form 1

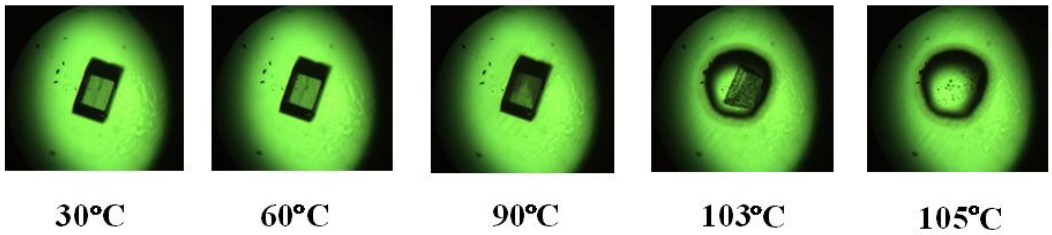

Form 2

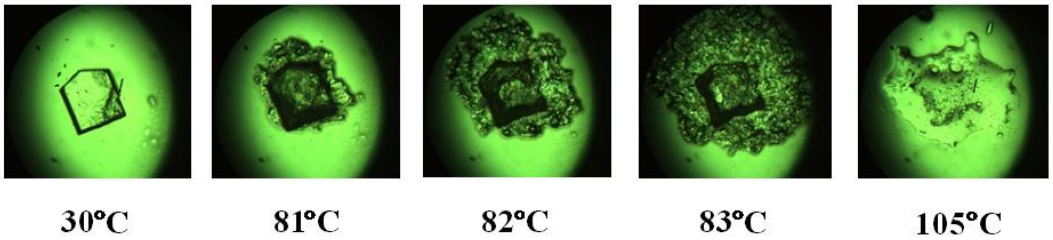

Fig. S5 HSM snapshots of SACT−ACT cocrystal polymorphs. Significant morphological changes were observed between 81-83 °C in form 2 whereas form 1 exhibited clean melting behavior.

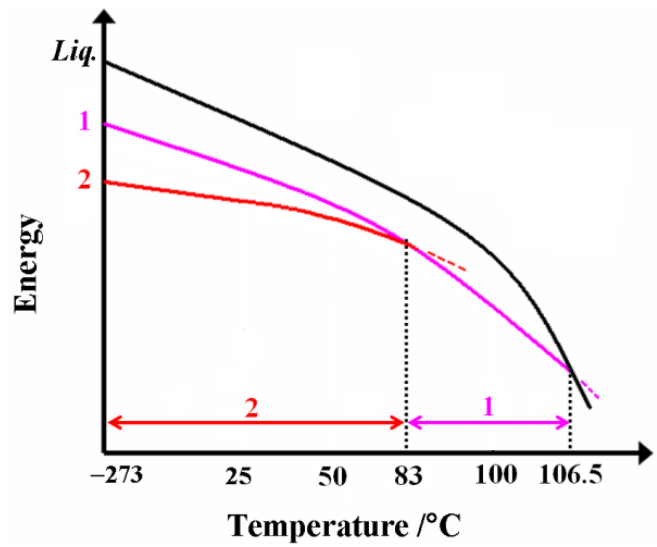

Fig. S6 Semi-quantitative E/T curves to show the stability of SACT−ACT polymorphs. Form 2 is the thermodynamic polymorph at absolute zero (−273 °C) and up to RT. Form 2 undergoes a phase transition at 83 °C to form 1. Form 1 is stable from 83 °C up to the melting temperature of 107 °C. Form 2 is stable between 25-83 °C, which is in agreement with the slurry and grinding experiments of form 1 converting to form 2, and form 2 being stable to these conditions. The dashed line indicates that the polymorph has transformed to another form at that temperature, T_{trs}.

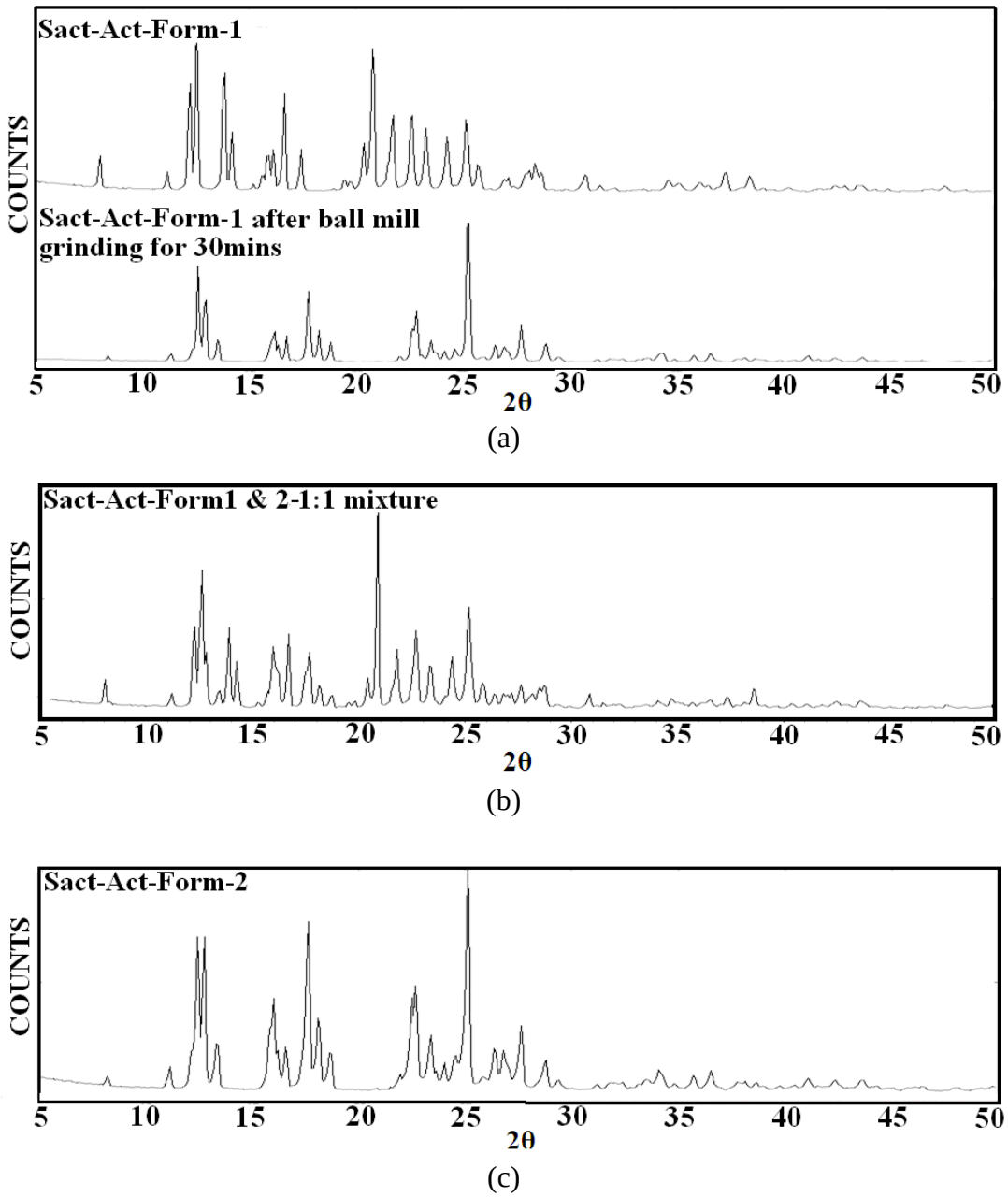

Fig. S7 (a) Experimental PXRD of SACT−ACT form 1 after neat grinding in ball mill for 30 min matches with that of form 2. There is no change for form 2. (b) Experimental PXRD of a 1:1 mixture of SACT−ACT form 1 and 2 converted to form 2 after neat grinding in ball mill for 10 min. (c) Experimental PXRD of SACT−ACT form 2 did not show any change after neat grinding in ball mill for 3 h.

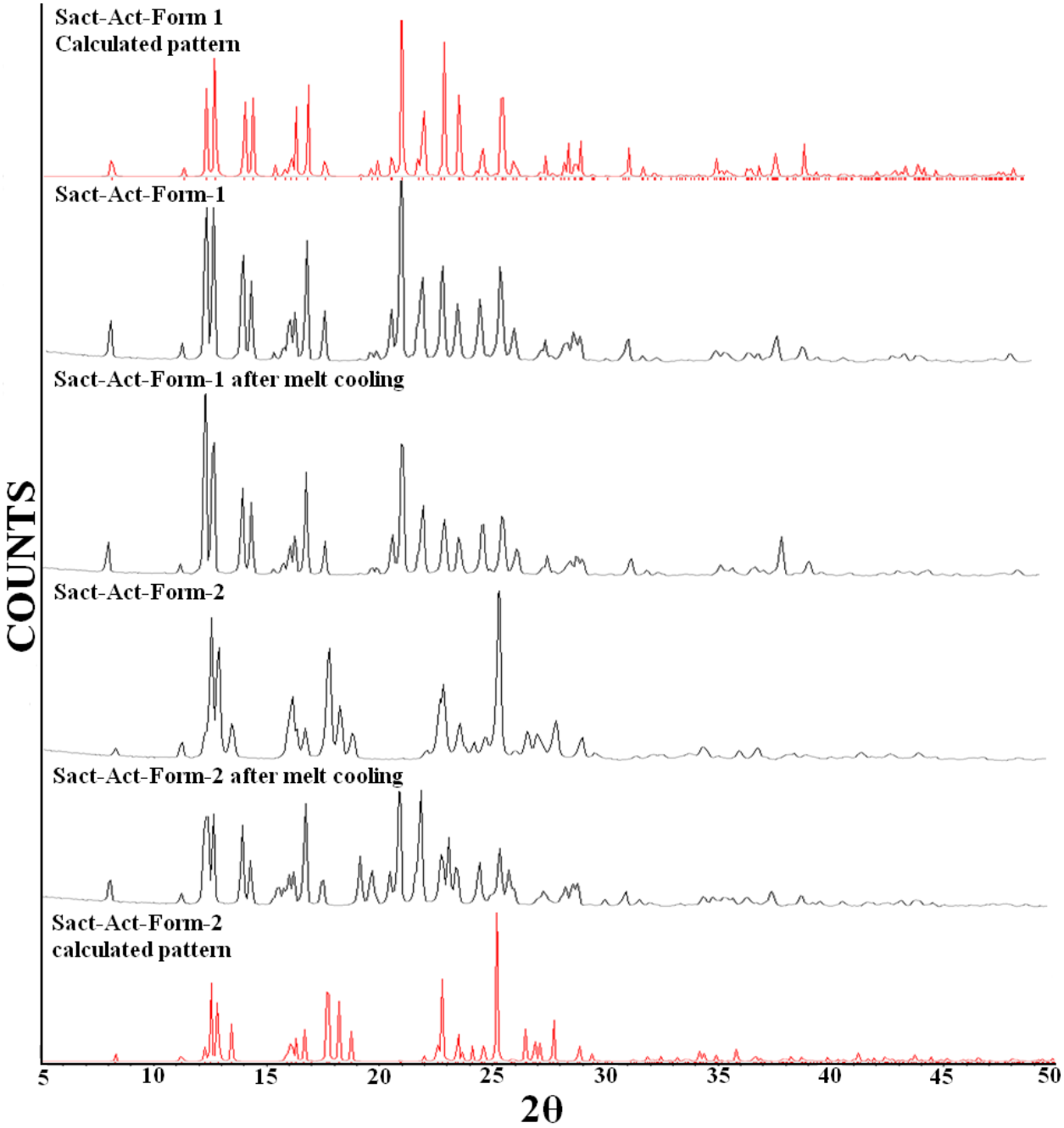

Fig. S8 Melt cooling of SACT–ACT form 1 or form 2 resulted in the crystallization of form 1 in either case, consistent with the Ostwald's Law of Stages. Thus melt cooling establishes form 1 as the kinetic, metastable modification.

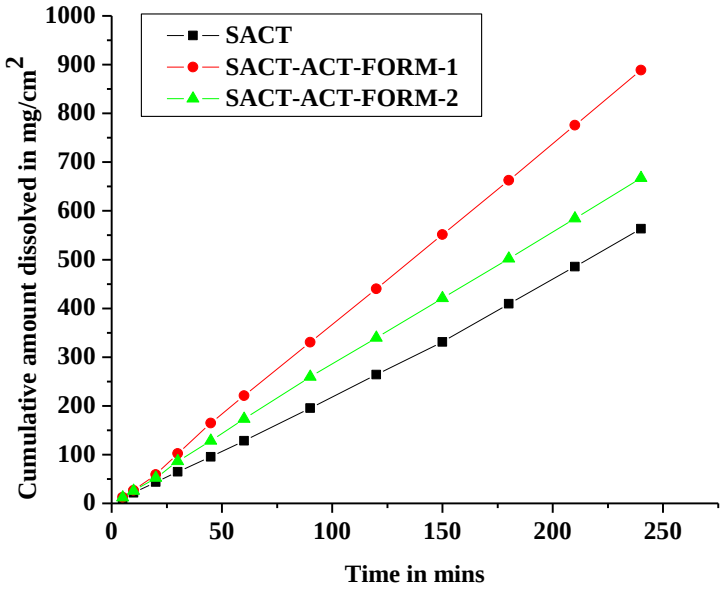

Fig. S9 IDR curves of SACT–ACT polymorphs in pH7 buffer medium.

Table S5 Intrinsic dissolution rates of SACT polymorphs along with their molar extinction coefficient (ε), and AUC values. The number of times enhancement of IDR and AUC with respect to SACT is given in parentheses.

Compound	Molar Extinction coefficient (/mM/cm)	Equi. Sol. (g/L)	IDR ($mg/cm^2/min$)	AUC_{0-4h} (mg h/L)
SACT	22.8	14.5	2.18	64,763
SACT–ACT form 1	17.9	--	3.4 (x 1.57)	105,679 (x1.63)
SACT–ACT form 2	19.9	--	2.8 (x 1.27)	80,853 (x1.25)

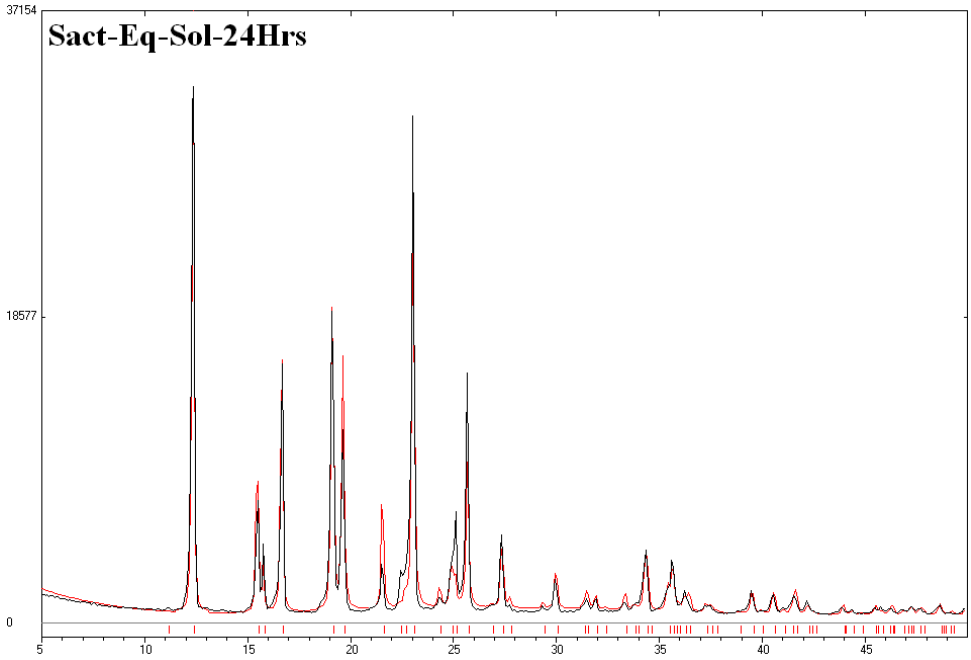
Sact-Eq-Sol-24Hrs
37154
18577
0
5
10
15
20
25
30
35
40
45

(a)

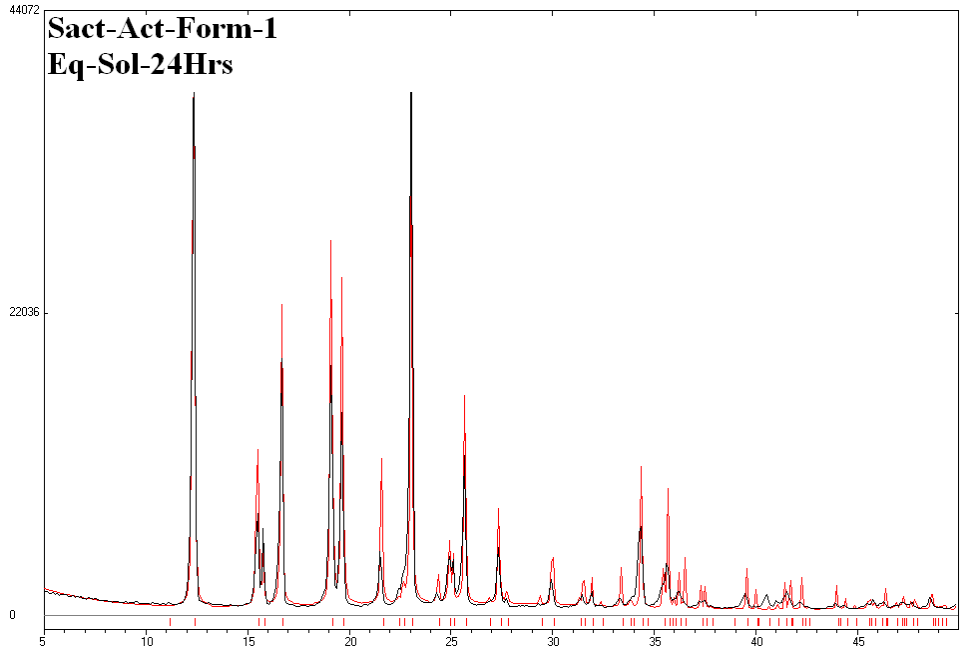
Sact-Act-Form-1
Eq-Sol-24Hrs
44072
22036
0
5
10
15
20
25
30
35
40
45

(b)

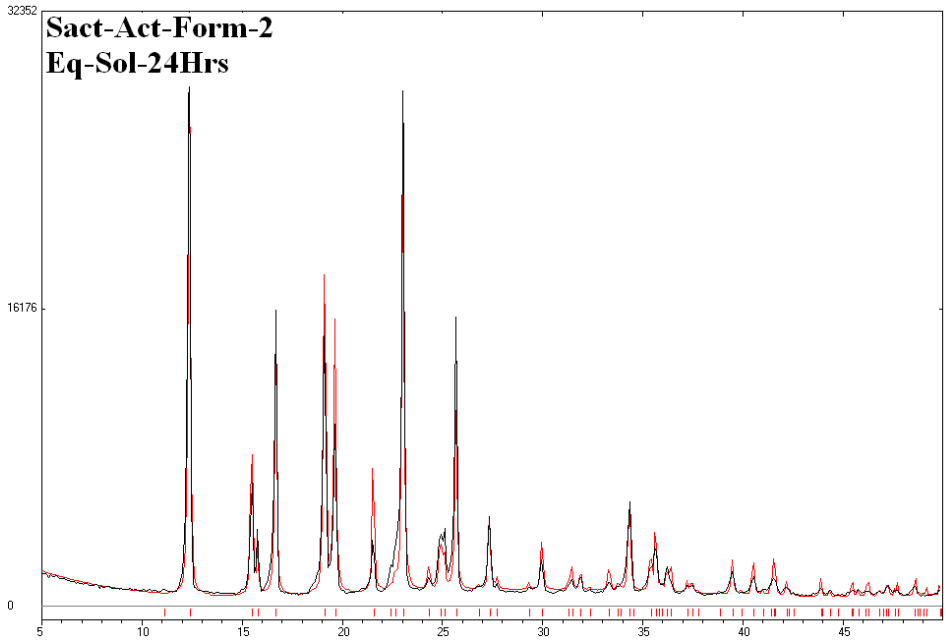

(c)

Fig. S10 Stability measurement at the end of the solubility experiment (24 h) in the slurry medium. (a) PXRD of SACT at the end of the equilibrium solubility experiment matches with the calculated XRD lines of the crystal structure, indicating form stability. (b) PXRD of SACT−ACT form 1 at the end of the equilibrium solubility experiment matches with the calculated XRD lines of SACT, indicating dissociation of the cocrystal. (c) PXRD of SACT−ACT form 2 at the end of the equilibrium solubility experiment (24 h) matches with the calculated XRD lines of SACT, indicating dissociation of the cocrystal

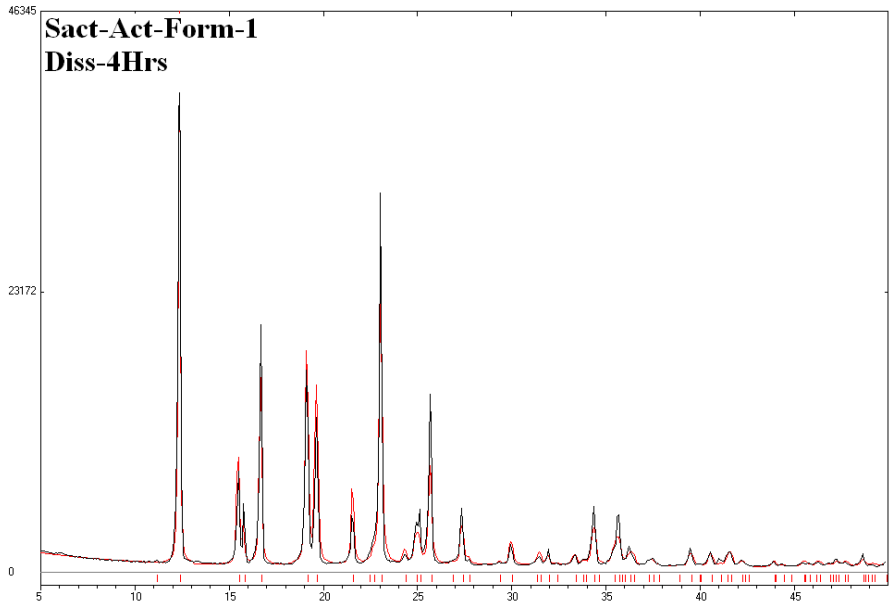

(a)

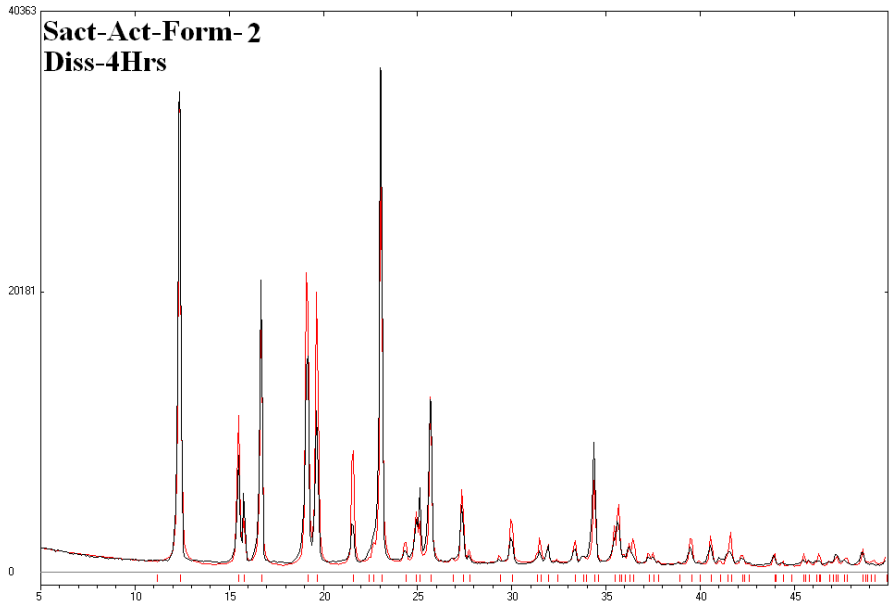

(b)

Fig. S11 PXRD plots of SACT and its cocrystal polymorphs at the end of the dissolution experiment (4 h). (a) PXRD of SACT−ACT form 1 at the end of the dissolution experiment (4 h) matches with the calculated XRD lines of SACT, indicating dissociation of the cocrystal. (b) PXRD of SACT−ACT form 2 at the end of dissolution experiment (4 h) matches with the calculated XRD lines of SACT, indicating dissociation of the cocrystal.

Experimental Section

Phase transformation experiments

Grinding experiments were done on 100 mg scale. Competitive grinding experiments were carried out on 1:1 stoichiometric ratio of the polymorphs (100 mg each). A Retsch mixer-mill equipped with a 5 mL stainless steel grinding jar and SS balls of 4 mm diameter was used for mechanical grinding. Slurry experiments were also done on 100 mg scale. Competitive slurry experiments were carried out on 1:1 stoichiometric ratio of the polymorphs (100 mg each). Toluene (5 mL in each experiment) was used as solvent in slurry experiments.

Single crystal X-ray diffraction

Crystal structures of the polymorphs were collected on CrysAlisPro, Oxford Diffraction Ltd., Version 1.171.33.55 with SCALE3 ABSPACK absorption correction, Xcalibur, EOS, Gemini measurement device and Mo-Kα (λ = 0.71073 Å) radiation.[1] Data reduction and structure refinement was performed using OLEX2 software.[2] Non-hydrogen atoms were refined anisotropically. C–H hydrogen atoms were positioned geometrically and refined in the riding model approximation. The methyl group in the ACT molecule has relatively large ADPs due to libration of H atoms. Attempts to split the electron density over two locations gave negative s.o.f. for the second C position, and so the process was abandoned. A check of the final CIF file using PLATON[3] did not show any missed symmetry. Hydrogen bond distances shown in Table 2 are neutron normalized to fix the D–H distance to its accurate neutron value in the X-ray crystal structures (O–H 0.983 Å, N–H 1.009 Å, and C–H 1.083 Å). After the final refinement, structure analysis and preparation of art works were carried out using MERCURY and X-SEED[4] software.

Vibrational spectroscopy

Thermo-Nicolet 6700 Fourier transform infrared spectrophotometer with NXR-Fourier transform Raman module (Thermo Scientific, Waltham, Massachusetts) was used to record IR and Raman spectra. IR was recorded on samples dispersed in KBr pellets. Raman spectra were recorded on samples contained in standard NMR diameter tubes or on compressed samples contained in a gold-coated sample holder. Data were analyzed using the Omnic software (Thermo Scientific, Waltham, Massachusetts).

Thermal analysis

Differential scanning calorimetry was performed on a Mettler-Toledo DSC 822e module (Mettler-Toledo, Columbus, Ohio). Samples were placed in crimped but vented aluminum pans for these experiments. The typical sample size is 3−5mg for the experiment. The temperature range for the heating curve was 30−150 °C and the sample was heated at a rate of 10°C/min. Samples were purged in a stream of dry nitrogen flowing at 80 mL/ min. Melting point of SACT-ACT form 2 was determined by heating the sample from 30−150 °C at a heating rate of 125 °C/min.

Powder X-ray diffraction

Powder X-ray diffraction of the polymorphs were recorded on Bruker D8 Focus diffractometer (Bruker-AXS, Karlsruhe, Germany) using Cu-Kα X-radiation (λ = 1.5406 Å) at 40 kV and 30 mA power. X-ray diffraction patterns were collected over the 2θ range 5–50° at a scan rate of 1º /min. Powder Cell 2.4 (Federal Institute of Materials Research and Testing, Berlin, Germany)[5] was used for Rietveld refinement of experimental PXRD and calculated lines from the X-ray crystal structure. VT-PXRD was performed on the same instrument equipped with a variable temperature stage -TTK450 module. PXRD patterns for both the forms were collected at 30, 60, 80, 86 and 92 ºC. All the powder patterns were plotted using Origin 7.0 software.

Hot stage microscopy

HSM was performed on a Wagner & Munz PolythermA Hot Stage and Heiztisch microscope. A Moticam 1000 (1.3 MP) camera supported by software Motic Image Plus 2.0ML is used to record images.

Solid-state NMR spectroscopy

Solid-state ^{13}C NMR spectra were recorded on Bruker Avance 400 MHz spectrometer (Bruker-Biospin, Karlsruhe, Germany). SS-NMR measurements were carried out on Bruker 4-mm double resonance CP-MAS probe in zirconia rotors with a Kel-F cap at 5.0-kHz spinning rate with a cross-polarization contact time of 2.5 ms and a delay of 8 s. ^{13}C NMR spectra were recorded at 100 MHz and referenced to the methylene carbon of glycine, and then recalibrated to the TMS scale ($\delta_{glycine}$ = 43.3 ppm).

Cambridge Structural Database

The CSD (version 5.34, ConQuest 1.15, November 2012 release)[6] was searched for cocrystal polymorphs. The parameters “all polymorphic structures with 3D coordinates determined”, “no errors”, “no polymeric”, and “no ions” were searched to give 6539 hits. Crystal structures were visualized with Mercury 2.0, and 72 sets of cocrystal polymorphs were manually retrieved (3D coordinates reported for all polymorph sets). Crystal structures with any degree of disorder were excluded. Details of polymorphic cocrystal sets are listed in the Supporting Information, Table S3.

Dissolution and Solubility measurements

The solubility curves of cocrystal polymorphs were measured using the Higuchi and Connor method[7] in pH 7 buffer medium at 30 °C. First, the absorbance of a known concentration of the polymorphs was measured at the given λ_{max} (SACT at 256 nm and SACT-ACT form 1 and 2 at 257 nm) in pH 7 buffer medium on Thermo Scientific Evolution 300 UV–vis spectrometer (Thermo Scientific, Waltham, MA). These absorbance values were plotted against several known concentrations to prepare the concentration vs. intensity calibration curve. From the slope of the calibration curves, molar extinction coefficients for the polymorphs were calculated. An excess amount of the sample was added to 6 mL of pH 7 buffer medium. The supersaturated solution was stirred at 300 rpm using a magnetic stirrer at 30 °C. After 24 h, the suspension was filtered through 0.45μ syringe filter. The filtered aliquots were diluted sufficiently, and the absorbance was measured at the given λ_{max}. IDR experiments were carried out on USP-certified Electrolab

TDT-08L dissolution tester (Mumbai, India). Dissolution experiments were performed for 4 hrs in pH 7 buffer medium at 37 °C. Prior to IDR estimation, standard curves for all the compounds were obtained spectrophotometrically at their respective λ_{max}. The calculated molar extinction coefficients were used to determine the IDR values. For IDR measurements, 500 mg of the compound was taken in the intrinsic attachment and compressed to 0.5-cm^2 disk using a hydraulic press 2.5 ton/in^2 pressure for 4 min. The intrinsic attachment was placed in a jar of 900 mL medium preheated to 37 °C and rotated at 150 rpm. 5 mL of the aliquot was collected at specific time intervals, and the concentration of the aliquots was determined with appropriate dilutions from the predetermined standard curves of the respective compounds. The IDR of the compound was calculated in the linear region of the dissolution curve (which is the slope of the curve or amount of drug dissolved/surface area of the disk) per unit time. The identity of the undissolved material after the dissolution experiment was ascertained by PXRD. The nature of the solid samples after disk compression and solubility/dissolution measurements were verified by PXRD.

References

1. CrysAlis CCD and CrysAlis RED, Versions 1.171.33.55, Oxford Diffraction, Oxford, 2008.
2. O. V. Dolomanov, L. J. Bourhis, R. J. Gildea, J. A. K. Howard and H. Puschmann, *J. Appl. Crystallogr.*, 2009, **42**, 339.
3. (a) A. L. Spek, PLATON: *A Multipurpose Crystallographic Tool*; Utrecht University: Utrecht, The Netherlands, 2002. (b) A. L. Spek, J. *Appl Crystallogr.*, 2003, **7**, 36.
4. (a) L. J. Barbour, *Supramol. Chem*. 2001, **1**, 189; (b) L. J. Barbour, *X-Seed, Graphical Interface to SHELX-97 and POV-Ray;* University of Missouri-Columbia: Columbus, MO, 1999.
5. Powder Cell, a program for structure visualization, powder pattern calculation and profile fitting. http://www.ccp14.ac.uk/tutorial/powdcell/.
6. Cambridge Structural Database, CSD, version 5.34, ConQuest 1.15, Nov 2013 update.
7. T. Higuchi and K. A. Connors, *Adv. Anal. Chem. Instrum*., 1965, **4**, 117.